Shawky et al., J Nanosci Curr Res 2016, 1:1
DOI: 10.4172/2572-0813.1000103

Journal of Nanosciences: Current Research

Research Article Open Access

Efficient Loading and Encapsulation of Anti-Tuberculosis Drugs using Multifunctional Mesoporous Silicate Nanoparticles

Sherif M. Shawky[1,2], Ahmed A. Abo-AlHassan[3], Holger Lill[4], Dirk Bald[4], Sherif F.EL-Khamisy[2,5], El-Zeiny M. Ebeid[1,3*]

[1]*Biochemistry Department, Misr University for Science and Technology, Egypt*
[2]*Center of Genomics, Helmy Institute, Zewail City of Science and Technology, Egypt*
[3]*Chemistry Department, Tanta University, Egypt*
[4]*Faculty of Earth and Life Sciences, Department of Molecular Cell Biology, Vrije Universiteit Amsterdam, Netherlands*
[5]*Krebs Institute, University of Sheffield, Sheffield, S10 2TN, UK*

Abstract

Objectives: Development of a novel method for loading drugs into spherical mesoporous silicate nanoparticles (MSNs), and further modification for the loaded MSNs to produce smart drug delivery system.

Methods: MSNs have been prepared and loaded using rotary evaporation as a novel method for drug loading. The highly loaded MSNs were further modified as a smart drug delivery system designed for endosomal escape, and sustained release of its cargo into the cytosol. MSNs loaded with anti-tuberculosis front line drugs such as isoniazid, pyrazinamide, pyrazonic acid, and ethambutol, in addition to fluorescein, have been coated with polyethyleneimine followed by mannose labeling for selective targeting of macrophage cells, the loading efficiency was compared to the conventional impregnation loading method. The selected drugs exhibit differences size, charge, and polarity. The developed delivery system has been characterized to indicate the surface are, loading efficiency, morphology, and release behavior at different pH.

Results: The loading process is independent of the nature of the drug molecule used and achieves loading efficiencies reaching one order of magnitude higher than those reported for conventional impregnation loading method. Characterization of the modified system indicated unique high surface area as high as 875.8 m^2/g, pore size of 3.86 nm, and total pore volume of 1.029 cm^3/g. *In-vitro* release experiments confirmed the pH-controlled release of the cargo molecules from the nanoparticles.

Conclusion: We have concomitantly employed previously reported components such as mesoporous silicate, polyethyleneimine coating and mannose labeling, in addition to a novel encapsulation method combined together to develop a smart drug delivery system making use of the advantages of each component. The developed system may be used as a potential novel drug delivery system for combating tuberculosis and/or alike clinical disorders.

Keywords: Drug loading efficiency; Thermo-gravimetric analysis; Anti-tuberculosis drugs; Fluorescein; Polyethyleneimine (PEI); *In-vitro* release kinetics

Introduction

One of the most challenging issues facing the pharmaceutical industry today is selective delivery of drugs and/or genes to the diseased cells [1]. Selective targeting permits the use of lower drug doses and consequently minimizes toxic side effects [2]. Nanoparticles (NPs) are widely used for a broad spectrum of applications in biomedicine, such as drug delivery and medical diagnostics. Mesoporous silica nanoparticles are of great interest as efficient drug/gene delivery systems due to their unique properties such as large surface area, tunable pore sizes, highly ordered structures in addition to their chemical and thermal stability [3]. Moreover, mesoporous silicate nanoparticles have high loading efficiency for both hydrophilic and hydrophobic molecules [4,5]. In addition, they have been previously used in controlled drug release [6].

Novel approaches and strategies are urgently needed to improve current tuberculosis (T.B) chemotherapy [7] and efforts are directed towards shortening and simplifying tuberculosis treatment [8,9]. Nanoparticle (NP) - based drug delivery systems for the current anti-TB drugs carriers have been previously used and developed with the aim to improve and simplify TB chemotherapy [10]. Despite the high efficiencies reported for these NP- based carriers [11,12], most of them still lack the properties of an ideal delivery system combining ease of synthesis, high drug loading efficiency, tunable surface properties, high surface area, controlled drug release, and cell-specific targeting, which has been found in the mesoporous silica NPs [13]. These features make NPs ideal for encapsulating different guest molecules and facilitate a wide range of applications such as drug and/or gene delivery in animal and plant cells [3]. In this communication we report a smart drug delivery system capable of encapsulating front line anti-tuberculosis drugs, which consists of MCM-41 mesoporous silicate nanoparticles loaded with anti-TB front line drugs, coated with cationic polymer PEI for pH control release of the drugs and decorated with mannose macrophage specific targeting moiety. PEI can assist in particles escaping from the endosomal vesicle after receptor mediated endocytosis. The low pH of the endosome lead to protonation of the amine groups located on PEI with subsequent swelling of the PEI coating and endosomal vesicle rupture leading to release of the drug particles into the cytoplasm [14,15]. Mannose molecules were used to functionalize the nanoparticles surfaces because of mannose ability to specifically target wide variety of macrophage cells expressing mannose specific membrane receptors. Consequently, delivery system bearing mannose moiety is internalized via receptor mediated endocytosis

***Corresponding author:** Prof. Dr. El-Zeiny M. Ebeid, Chemistry Department, Faculty of Science, Tanta University, Tanta, Egypt, 31111, Tel: 00201155000056, 002-0403318302; E-mail: elzeiny.ebeid@science.tanta.edu.eg

Received: May 27, 2016; **Accepted:** June 27, 2016; **Published:** July 07, 2016

Citation: Shawky SM, Abo-AlHassan AA, Lill H, Bald D, EL-Khamisy SF (2016) Efficient Loading and Encapsulation of Anti-Tuberculosis Drugs using Multifunctional Mesoporous Silicate Nanoparticles. J Nanosci Curr Res 1: 103. doi: 10.4172/2572-0813.1000103

[14,16-20] (Figure 1). *In vitro*-release kinetics at different pHs was assessed using fluorescein molecules.

Materials and Methods

Synthesis of mesoporous silica nanoparticles

Mesoporous silica nanoparticles (MSN) were synthesized as previously described [21,22]. Typically, 1 g of cetyltrimethyl ammonium bromide (CTAB) was dissolved completely in 480 ml deionized water with slight stirring till clear solution was obtained. Then, 3.5 ml of 2M sodium hydroxide was added and stirred vigorously at 80°C. After stabilization of the temperature at 80°C, 5 ml of tri-ethoxy-ortho-silicate (TEOS) were added drop-wise at a rate of 1 ml per minute, and the mixture was stirred vigorously for 2 hours. The white precipitate obtained was filtered, washed with methanol and water, and then dried at 100°C overnight.

Removal of surfactant

The dried powder was refluxed for 24 hours at 50°C in 100 ml methanol with 1 ml concentrated HCl. Then, the template (CTAB) was removed and the MSN were isolated via filtration, followed by extensive washing with water and methanol and then dried at 100°C for 24 hours.

Particles characterization

Scanning electron microscopy (SEM): The morphology and size of the prepared mesoporous silica nanoparticles were analyzed using field emission scanning electron microscope (SEM, LEO SUPRA 55; Carl Zeiss AG, Oberkochen, Germany). A small portion of the powder was fixed on SEM stage using carbon tape. The SEM micrographs were operated at 12 keV.

High resolution transmission electron microscopy (HRTEM): High resolution transmission electron micrographs were recorded on an HRTEM (JEM-2100) apparatus operating at 200 kV coupled with high resolution CCD Galatan digital camera for image processing of the mesoporous ordered structure of the prepared particles. A small portion of the produced particles were suspended in 1 ml acetone and sonicated for 3 minutes and then one drop was placed on the TEM carbon grid and analyzed by TEM.

Fourier- transform infrared spectroscopy (FT-IR): Fourier transform infrared spectroscopy (FT-IR) was used to record the IR spectra of the samples using potassium bromide (KBr) pellet technique. A small portion of the sample was mixed well with small portion of KBr powder in a mortar and then the mixture was analyzed by FT-IR Thermo-Nicolet FTIR Avatar 370.

Nitrogen adsorption/desorption isotherms: Surface area, pore size and pore volume of the prepared mesoporous silicate nanoparticles dried at 300°C for 8 h under vacuum were measured by nitrogen adsorption/desorption isotherms at - 196.14°C using Quantachrome Nova station instrument, version 10 analyzer. Specific surface area (SBET) was calculated using multi-point adsorption data from linear segment of the N2 adsorption isotherms using Brunauer-Emmett-Teller (BET) theory. On the other hand, the pore volume and pore size distribution were determined from the adsorption isotherms by using nonlocal density functional theory (NLDFT).

X-ray diffraction (XRD): The free and loaded particles were analyzed by an X- ray diffractometer **(Diffrac plus v1.01)** over the range of 0-80° with Cu anode at 40 kV and 30 mA, at 2 theta scale and wavelength 1.54 Å.

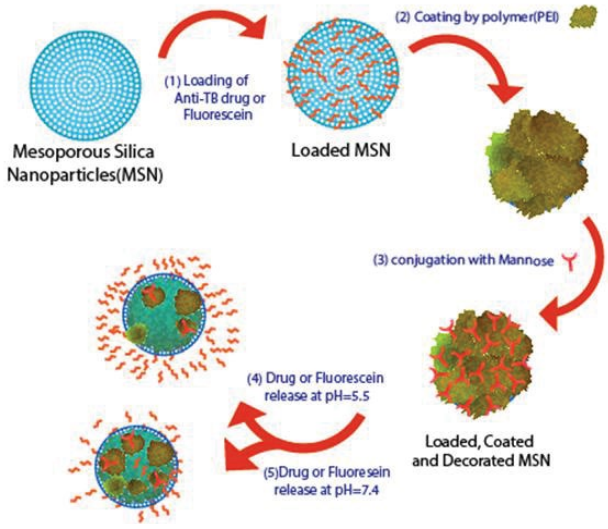

Figure 1: Illustration of the applied multifunctional mesoporous silicate nanoparticles components. Mesoporous silicate nanoparticles are firstly loaded with an anti-TB. drug or fluorescein using the rotavap technique. Secondly, the loaded particles are coated with Polyethylimine (PEI) polymer by the rotavap method. Thirdly, functionalized mannose (the manno-pyranosyl-phenyl-iso-thiocyanate mannose) molecule is conjugated to the loaded coated nanoparticles through the reaction of its phenyl isothiocyanate with the primary amine groups on PEI forming iso-thiourea linkage.

Encapsulation of anti-tuberculosis drugs and fluorescein

Two different methods have been used for loading the drugs into the prepared mesoporous nanoparticles. The first conventional method is impregnation of the MSN particles after dispersing them in the drug solution (15 mg drug/ml solvent) and stirring for about 72 hours. The solvent used differs from one drug to another (POA, fluorescein and isoniazid were dissolved in water, while PZA and ethambutol were dissolved in absolute ethanol) The MSN particles were dispersed in the drug solution by sonication for at least 10 minutes and then the mixture was stirred for 3 days. The particles were then filtered by 0.2 μm nylon membrane filters, dried at 50°C overnight. The amount of the drug taken by the particles was measured by thermo-gravimetric analysis (TGA).

The second method (rotavap method) was done by first preparing the drug solution in an appropriate solvent (15 mg drug/ml solvent). The solvents used here for each drug were the same as those used in the impregnation method. The MSN particles were dispersed in the drug solution by sonication for about 10 minutes. Then, the mixture (drug solution/MSN) was applied to the rotavap for 3 days till the solvent was evaporated completely. Finally, the dried particles were washed thoroughly to remove the unbound and the loosely bound drugs on the particles surface. The amount of the drug taken by the particles was measured by TGA.

Synthesis of polyethyleneimine (PEI) conjugated to mannopyranosyl phenyl iso-thiocyanate (Mannose)

Conjugation of PEI to mannose was done as previously described [15] with slight modifications. Briefly, branched PEI 25 kDa (40 mg) was mixed with 1 ml dimethyl sulfoxide (DMSO) by sonication for about 30 minutes and then the manno-pyranosyl-phenyl-iso-thiocyanate previously dissolved in DMSO (5 mg/0.5 ml) was added to the PEI solution. The reaction mixture was stirred at room temperature for one

day. Then, the PEI conjugated to mannose was purified by adding 5 ml of 0.5 M saline solution and dialyzed against 150 mM sodium chloride as described previously [14,15]. The amount of mannose conjugated to the PEI was calculated and determined by resorcinol-sulphuric acid test as previously described [23].

Coating the encapsulated particles with the mannosylated-polyethyleneimine (PEI)

For each drug batch, 150 mg of the loaded particles were dispersed in 10 ml absolute ethanol by sonication for 5 minutes, and then added to 5 ml of the mannose-PEI solution then further sonicated for about 5 minutes. Afterwards, the mixture was rotary evaporated for 2 hours at 50º C. The powder was then washed with absolute ethanol, filtered and dried.

Thermo gravimetric analysis (TGA)

The loading efficiency was tested by TGA. Particles loaded with different drugs were analyzed by TGA instrument (TGA Q50 V20.10 Build 36) by heating the particles from the ambient temperature to 1000°C at a heating rate of 10°C per minute using nitrogen as the purge gas at a flow rate of 100 ml per minute.

In vitro- pH controlled release kinetics

The *in-vitro* controlled release kinetics was studied at two different pH values. Briefly, 10 mg of MSN particles loaded with known amount (concentration) of fluorescein and coated with PEI were dispersed in two beakers (5 mg in each beaker) containing simulated body fluid (SBF), one with pH 5.5 (corresponding to the endosomal vesicle pH), while the other with pH 7.4 (corresponding to the blood plasma pH) and stirred. Every 3 hours, the solution was centrifuged and absorbance of fluorescein at 490 nm was recorded in the supernatant for each pH solution, then the precipitate was re-dispersed in SBF with the above-mentioned pHs. This process was done at different time intervals over a period of 70 hours. The absorbance was recorded by using a Shimadzu UV 160 A Spectrophotometer. The amounts of the fluorescein released were estimated using a previously plotted fluorescein absorbance standard curve. The total amount of released fluorescein was calculated cumulatively until the end of the experiment.

Results and Discussion

The drug delivery system that has been developed in this study is composed of mesoporous silicate nanoparticles (MCM-41 generation) loaded with selected anti-tuberculosis drugs of different sizes, charges, and polarities (ethambutol, isoniazid, pyrazinamide and Pyrazonic acid) in addition to fluorescein as a fluorescent tagging molecule. The loaded particles were then coated with the highly cationic polymer polyethyleneimine (PEI), for the pH-controlled release of cargo molecules. The adsorption of PEI onto the silica surface was done electrostatically as described before [24-26]. Finally, the particles have been decorated with mannose as a macrophage cells specific moiety [15]. The conjugation of PEI to the sugar molecule is based on the interaction of the iso-thiocyanate functional group in the mannose molecule with the primary amino groups distributed on the PEI polymer surface forming a strong amide bond as described in the materials and methods. Scanning electron microscope images (Figures 2 and 3) revealed that the prepared mesoporous silicate nanoparticles are mono distributed spheres with an average diameter of 90 to 100 nm, which is consistent with previous studies [4,27]. Moreover; TEM image (Figure 4) shows a honeycomb porous structure (ordered pores hexagonal packed channels).

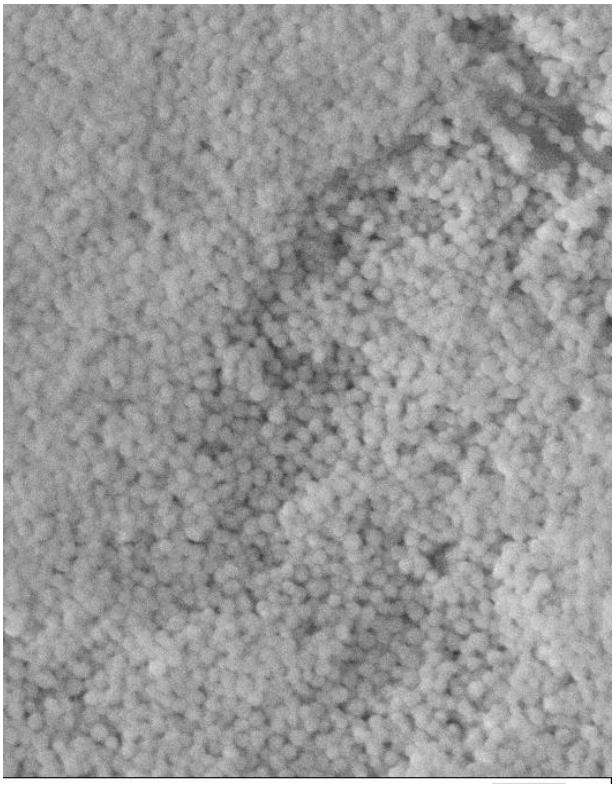

Figure 2: Scanning electron microscopy (SEM) image of mesoporous silica nanoparticles showing their size and morphology.

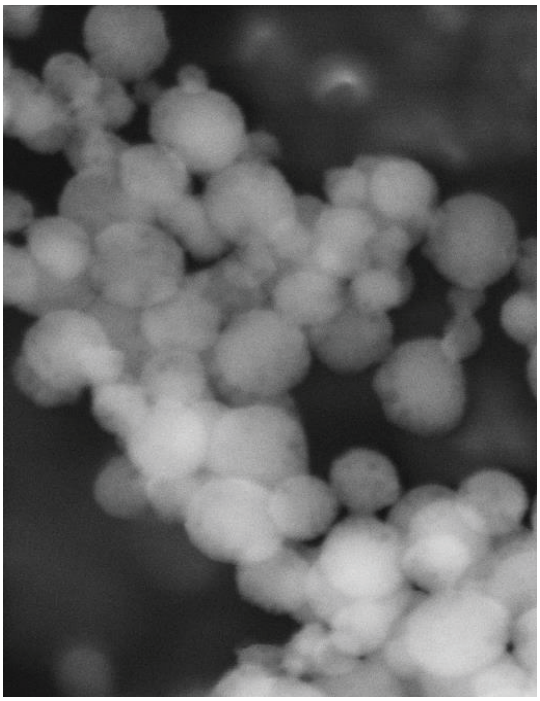

Figure 3: Scanning electron microscopy (SEM) image of mesoporous silica nanoparticles showing their uniform size and shape. The particles have an average diameter of 90 to 120 nm.

The nitrogen isotherm shown in Figure 5A is of type IV which is typical of mesoporous materials that have pores between 2- 50 nm, according to the (IUPAC) classification. There are two capillary condensation steps at P/Po at about 0.3 - 0.4 and P/Po at about 0.9, which correspond to the mesoporous and textual porosity produced by the inter-particles packing [5,27]. The N2 adsorption/desorption isotherms (Figure 5A) revealed a high surface area (SBET) of 875.8 m^2/g.

A narrow Barrett-Joyer-Halenda (BJH) pore size distribution (Figure 5B) has been obtained, with average pore size distribution of 3.86 nm, and a total Pore Volume of 1.029 cm^3/g. FT-IR spectra of the prepared particles were measured over the range 4000 to 400 cm^{-1}. The as-prepared particles spectrum is shown in Figure 6 which is typically of the MCM-41 particles as shown in previous studies [27,28]. The Si-O rocking vibration and Si-O bond stretching of surface Si-OH groups are shown at 460 cm^{-1} and 967 cm^{-1} respectively. Also, the very broad (hydrogen bonded) hydroxyl stretching band for both silanol Si-O-H and the water hydroxyls was clear at 3500 cm^{-1} in addition to the characteristic H-OH water twisting band at 1640 cm^{-1}. Also, the internal Si-O-Si stretching vibration of SiO_4 asymmetric band appeared at 1100 cm^{-1}, while the symmetric one is at 800 cm^{-1}. The silicate network is formed of Si-O-Si and plenty of silanol Si-OH groups (both internal and external ones) of different types as described elsewhere [27,29].

The MCM-41 generation of mesoporous silicate nanoparticles has 3 characteristic peaks pattern in the XRD analysis that is considered as a finger print for the MCM-41 mesoporous silica [6,22,27]. A strong reflection peak at 2.6° is related to the 100 plane and the two weak reflection peaks at 4.4° and 5.1° are related to 110 and 200 planes respectively. Loading or filling the pores of the particles with a cargo molecule (anti-TB drugs or fluorescein), have led to a significant decrease in intensity of the 2.6° peak and a small shift may also occur. On the other hand, the 4.4° and 5.1° peaks are related to the ordered structure of the synthesized material. In this study, we are highly interested in the 2.6° peak resolution for the determination the loading efficiency of the particles. The 2.6° peak decline indicates and confirms that the hexagonal pores of the particles are filled with

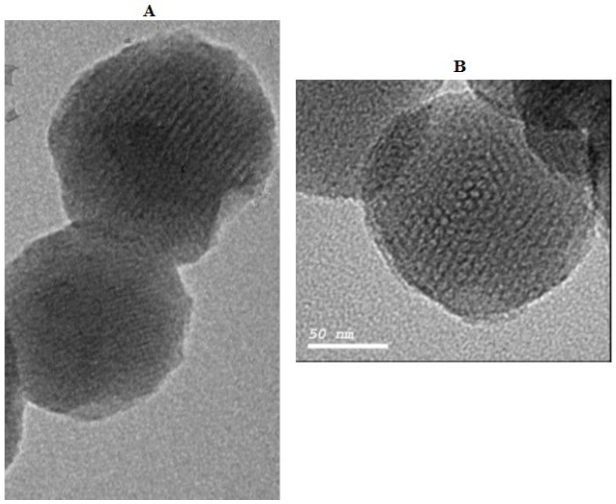

Figure 4: Transmission electron microscopy (TEM) images of mesoporous silica nanoparticles showing: **(A)** The honeycomb porous structure. The hexagonal straight channels are shown extending along the spherical particles. The particles have straight one dimensional cylindrical pores. **(B)** A top view of the particles showing the channels as a honey comb cage.

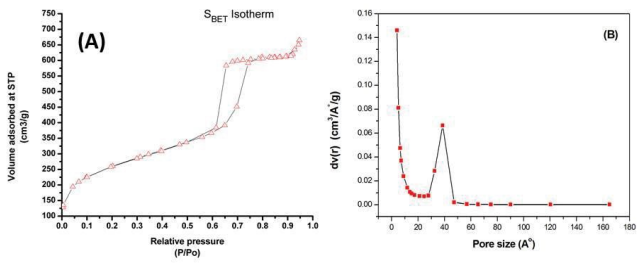

Figure 5: (**A)** Surface analysis by nitrogen sorption isotherms allowing surface area calculation by BET method. **(B)** The pore size of the prepared particles calculated by the Barrett-Joyer-Halenda (BJH) method.

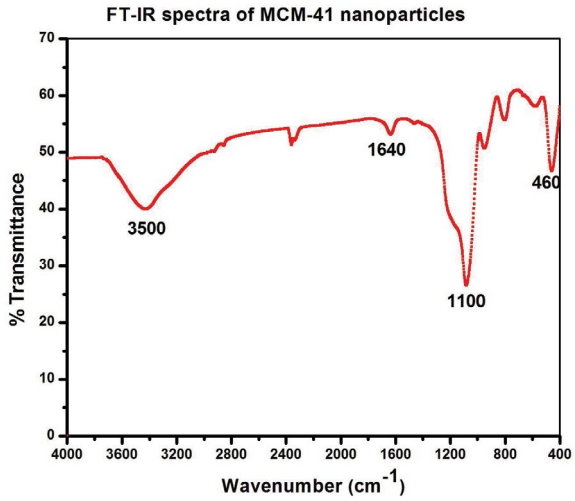

Figure 6: FT-IR spectra of the mesoporous silica nanoparticles using potassium bromide (KBr) pellet technique.

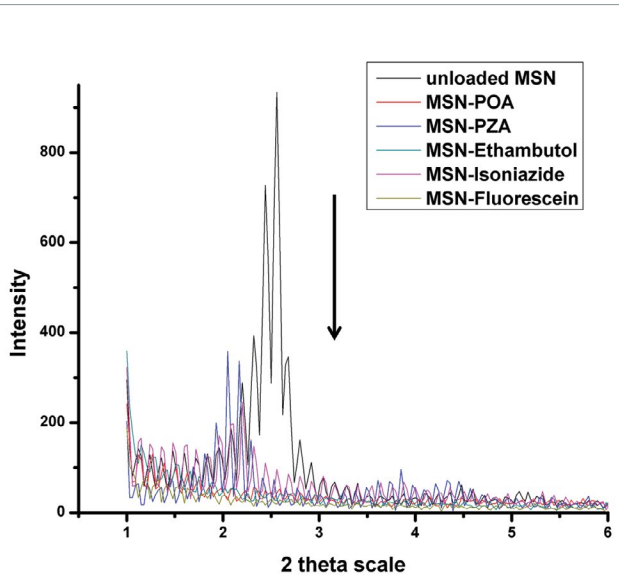

Figure 7: X-ray diffraction analysis of unloaded mesoporous silica and particles loaded with Pyrazonic acid (POA), pyrazinamide (PZA), ethambutol, isoniazid and fluorescein.

different drug molecules. Also, the 2.6° peak and its value have been used in Bragg's and Scherer's formulas. According to the reflection peak of the unloaded mesoporous silica nanoparticles shown in Figure 7, the following calculations were done [4,6,27]. The (d100) for the unloaded particles was calculated from Bragg's formula as d100 = 3.44 nm (2θ angle = 2.56°, λ = 1.54 nm). This value is consistent with other studies stating that the d100 inter-particles plane distances is almost between 3 and 4 nm for the unloaded MCM-41 generation [4-6,27,30].

The pore center distance, which is the pore size distribution (Å) = 2 d100/√3= 3.972 nm, a value that is almost the same obtained by the N2 adsorption-desorption as 3.86 nm (Figure 4B).

Drug loading efficiency

The main core of this study is to develop a method for high loading efficiency applying molecular encapsulation into MSN. We loaded the NPs with three drugs currently in use as anti-tuberculosis chemotherapy namely isoniazid, ethambutol and pyrazinamide. As pyrazinamide is a pro-drug that needs to be hydrolyzed for antibacterial activity we also included its active entity, pyrazonic acid. Two drug loading strategies have been adopted in this study via impregnation and rotavap procedures. TGA was employed to determine the loading efficiencies. Figures 8-12 describe the TGA thermograms of the drugs loaded by the rotavap method, while Figures S1-S5 (supplementary info) show the TGA of the same drugs loaded by the conventional impregnation method. The TGA experiments were done prior to application of PEI / mannose coatings in order to exclude any interference that may occur by the PEI and/or mannose molecules in the data analysis.

There are three main weight loss steps in the TGA curves of loaded MCM-41 that goes in agreement with earlier studies [27,29]:

1- Initial weight loss below 100°C of adsorbed moisture and solvent.

2- Step I commencing at ca. 200°C that is assigned to decomposition of the surface bound functional groups such as amino and thiol groups.

3- Step II occurring at 250- 450°C that is assigned to decomposition of the functional groups e.g.: amino groups bound to the inside pore walls.

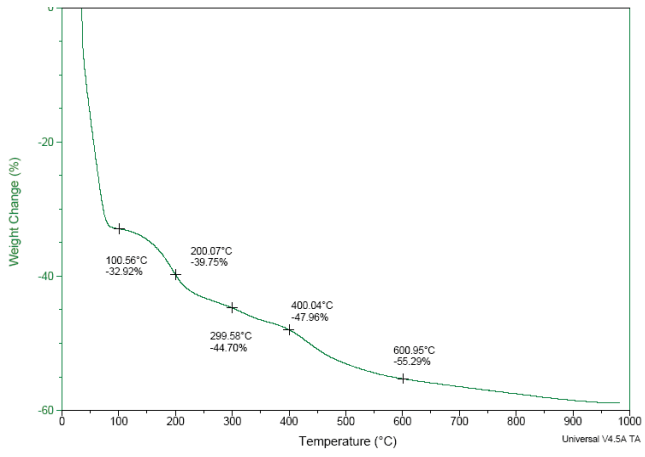

Figure 8: TGA curve of nanoparticles loaded with pyrazonic acid (POA) using rotavap method showing the weight loss below 100°C, and the weight loss between 100°Cand 600°C. The experiment was done in duplicates with a standard deviation of 1.7.

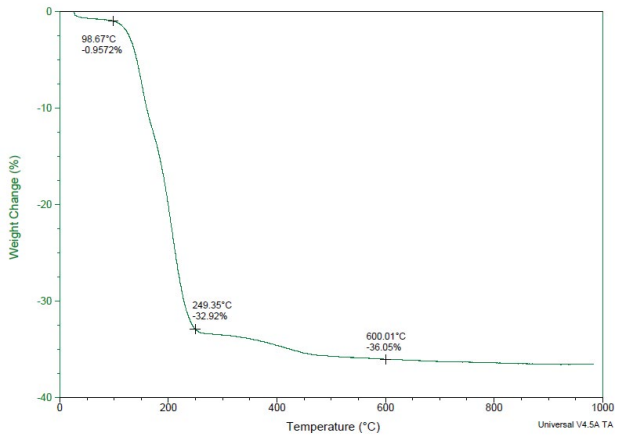

Figure 9: TGA curve of nanoparticles loaded with pyrazinamide (PZA) using rotavap method showing the weight loss below 100°C, and the weight loss between 100°C and 600°C. The experiment was done in duplicates with a standard deviation of 2.1.

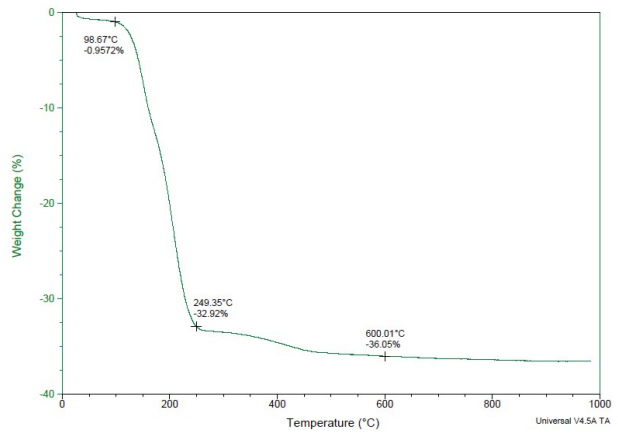

Figure 10: TGA curve of nanoparticles loaded with isoniazid using rotavap method showing the weight loss below 100°C, and the weight loss between 100°C and 600°C. The experiment was done in duplicates with a standard deviation of 2.8.

4- Step III occurring above 600°C that is related to the dehydration (decomposition) of the particle's silanol groups.

So, the amount of drugs loaded within the particles could be estimated by the weight loss between 100 to 600°C. The amounts of the loaded drugs are given in Table 1.

According to data in Table 1, all four drugs and fluorescein were successfully encapsulated into the NPs. The loaded amounts of the drugs used herein were considerably high upon using the rotavap method compared to the conventional impregnation method.

The loaded amounts also exceeded early reported values for isoniazid and rifampicin reported earlier by Zhu et al. as 37.89 and 3.77 μg/mg MSN respectively [31].

Further advantage of the rotavap method is the independence of the drug class, charge and size.

Controlled release of fluorescein

Loaded drug	Impregnation method			Rotavap method		
	Weight loss % (100℃ to 600℃)	Amount of loaded drug in µg / mg MSN	Standard deviation	Weight loss % (100℃to 600℃)	Amount of loaded drug in µg / mg MSN	Standard deviation
Isoniazid	6	28.8	1.7	40	400	2.8
Pyrazinamide	8.9	106.8	2.1	35	350	2.1
Pyrazonic acid	6.5	90.6	2.8	22.5	225	1.7
Ethambutol	5	12.5	1.4	12	120	1.4
Fluorescein	6	75	1.4	22.2	221	1.4

Table 1: Comparison between the loading amount efficiency of the selected drugs as estimated by TGA for the rotary- evaporator and the impregnation methods. The experiments were carried out in duplicate.

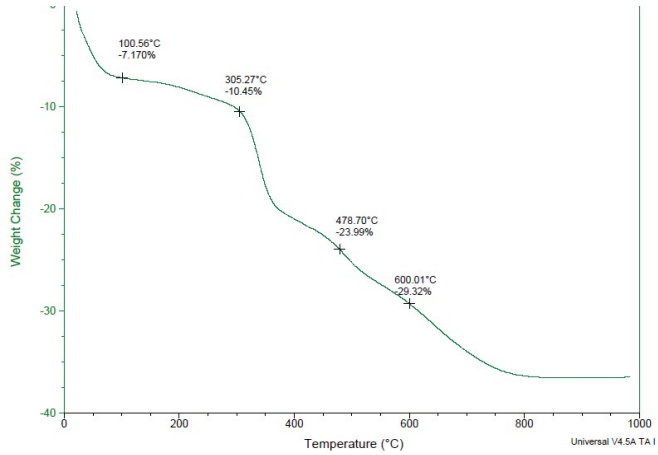

Figure 11: TGA curve of nanoparticles loaded with fluorescein using rotavap method showing the weight loss below 100°C, and the weight loss between 100°C and 600°C.The experiment was done in duplicates with a standard deviation of 1.4.

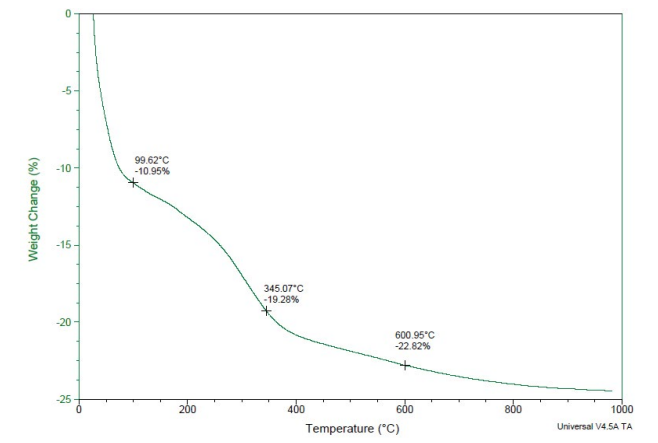

Figure 12: TGA curve of nanoparticles loaded with ethambutol using rotavap method showing the weight loss below 100°C, and the weight loss between 100°C and 600°C.The experiment was done in duplicates with a standard deviation of 1.4.

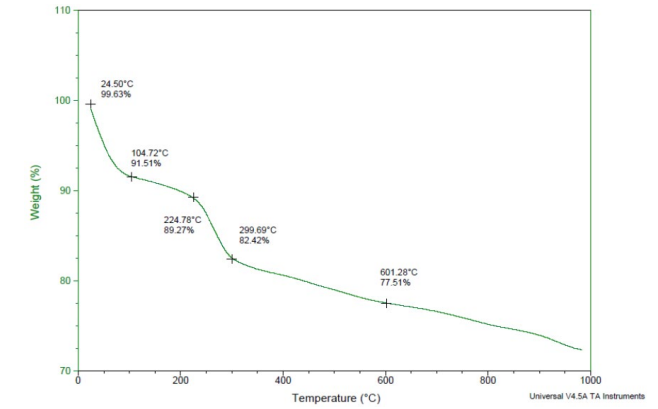

Figure S1: TGA of nano particles loaded with pyrazonic acid (POA) using impregnation method showing the weight losses below 100°C, and in the temperature range 100°C - 600°C.

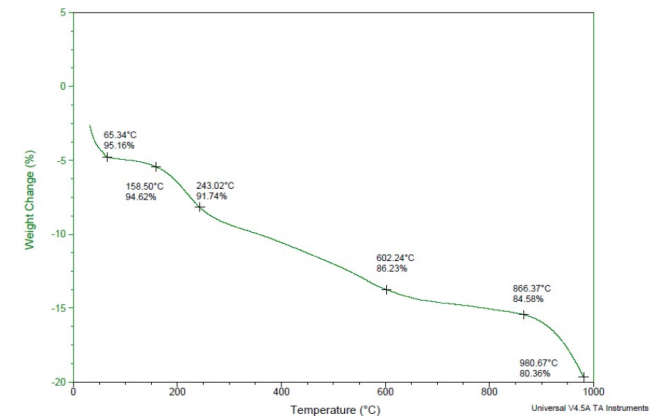

Figure S2: TGA curve of nanoparticles loaded with pyrazinamide (PZA) using impregnation method showing the weight losses below 100ºC, and in the temperature range 100-600ºC.

pH-stimulated release of NPs cargo is an important criteria since pathogenic bacteria such as TB bacteria (*Mycobacterium tuberculosis* and related bacteria) during infection, can be located in slightly acidic environments, e.g.: in inflammated tissues or in the endosome of human macrophage cells. The PEI-coating of the NPs described here is important for this purpose since PEI exhibits a proton sponge effect [32-34] which leads to endosomal vesicle rupture and thus preventing lysosomal degradation of the particles and leads to the particles liberation into the cytoplasm [22]. This behavior is due to the fact that acidic pH leads to protonation of the excessive imine groups on PEI as well as interaction with counter ions, and water molecules diffusion. Consequently, gradual PEI swelling and formation of open hole-like pores in the endosomal vesicle as a result of the osmotic pressure difference results in the liberation of the encapsulated particles with concomitant release of drugs into the cell's cytosol [15,35]. In the present study we demonstrated a cargo release from MSN, loaded with fluorescein coated with polyethyleneimine (PEI) in simulated Body Fluid (SBF) as a release medium at pH values of 7.4 and 5.5 to mimic blood plasma and the endosomal vesicles pHs respectively. After about

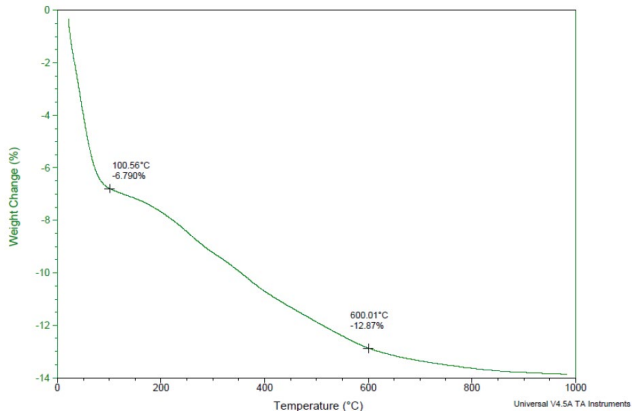

Figure S3: TGA curve of nanoparticles loaded with isoniazid using impregnation method showing the weight losses below 100ºC, and in the temperature range 100-600ºC.

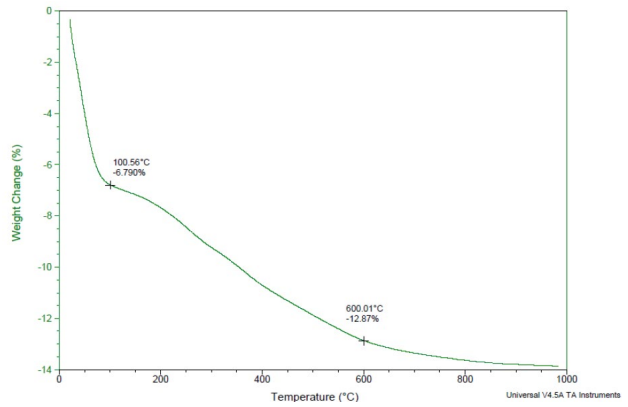

Figure S4: TGA curve of nanoparticles loaded with fluorescein using impregnation method showing the weight losses below 100ºC, and in the temperature range 100-600ºC.

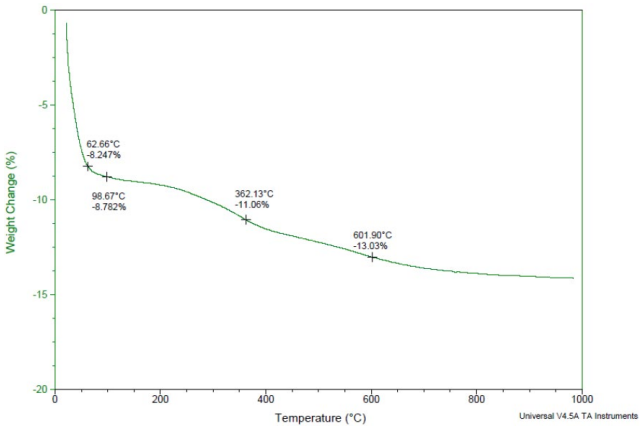

Figure S5: TGA curve of nanoparticles loaded with ethambutol using impregnation method showing the weight losses below 100ºC, and in the temperature range 100-600ºC.

70 hours, the release was found to be about 100% and 40% for pHs 5.5 and pH 7.4 respectively (Figure 13). This confirms the ability of PEI

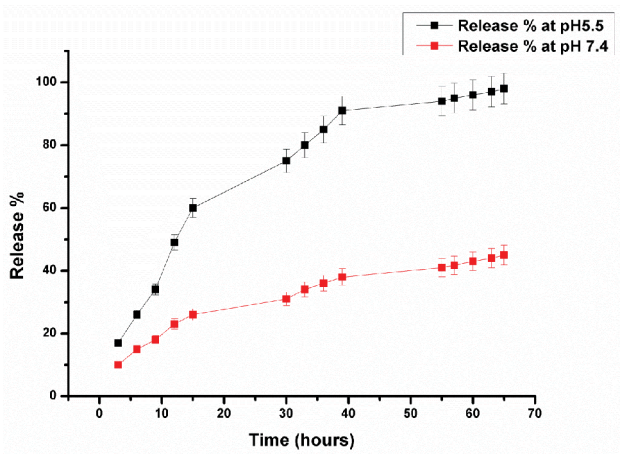

Figure 13: pH-controlled cargo release from nanoparticles assembly. The time course of fluorescein release from PEI-coated mesoporous silica nanoparticles was assessed by absorption spectrometry at 5.5 and 7.4 pH values.

to be used in pH-stimulated release of the drugs encapsulated within MSN.

Conclusion and Future Perspective

In this study, we have prepared MCM-41 mesoporous silica nanoparticles and encapsulated various anti-tuberculosis drugs as model molecules using an efficient rotavap method. The encapsulation efficiencies using the developed rotavap method were compared with the conventional loading impregnation method. The synthesis procedures for nanoparticles have been optimized to obtain large surface areas and controlled spherical shape. The rotavap technique for drug loading is a novel technique and, to our knowledge, has not been reported earlier for MSNs. Besides the high loading efficiencies, the rotavap method appears to be independent of drug nature, charge and solvent. The prepared MSNs have been further modified by coating with PEI linked to mannose as an endosomal escape and targeting moieties respectively. The multifunctional nanoparticles were characterized using SEM, TEM, FT-IR, XRD, and nitrogen adsorption/desorption isotherms for pore size/volume and surface area measurements. All the obtained results are consistent with previously reported studies [5,6,14,27].

Most known delivery systems cannot escape the endosomal vesicle after receptor mediated endocytosis and this leads to their degradation by the late endosome (lysosome). The NPs reported here are coated with PEI, which can assist in escaping from the endosome after endocytosis. The low pH values of the endosomal vesicle leads to the protonation of PEI with subsequent swelling of the PEI coating and endosomal vesicle rupture, leading to the release of the drug particles and the drugs into the cytoplasm [14,15]. From the release behavior of the fluorescein molecule from the nanoparticles assembly, a 2.5 fold percentage of the cargo release delay was recorded between plasma pH of 7.4 and endosomal vesicles pHs of 5.5. This becomes significant upon t using these particles *in vivo* allowing for prolonged circulation time in the blood. By this period of time, the particles are expected to find their way the desired cells because of their functionalization by mannose which is known as a targeting moiety to the macrophage cells [15]. Functionalization of the particles with other targeting molecules is also feasible.

As a follow-up to our study, the potential of our produced delivery

system for prevention of bacterial growth can be further evaluated, e.g. using a macrophage cell lines model. Tuberculosis bacteria can infect human alveolar macrophages and can survive in the phagosome of the host macrophages for an extended period, as a result of a prevention of the intracellular phago-lysosymal fusion [36]. The difficulty of the elimination of these intracellular bacteria significantly renders a prolonged TB chemotherapy (>6 months) [37]. The properties of the NP system reported here may prove useful for combating these recalcitrant pathogenic bacteria. Moreover, pyrazonic acid (POA) which is the active form of its pro-drug pyrazinamide (PZA) cannot diffuse into the human macrophage cells due to its negatively charged nature. This is why it is applied in the pyrazinamide form that is transformed to POA by the enzyme pyrazinamidase [37]. The main problem here is the appearance of drug-resistant strains that have mutations in the above mentioned enzyme and so the drug becomes ineffective. A nanoparticle system with encapsulated pyrazonic acid, as reported here, may turn out as promising system for direct delivery of the active drug entity into human cells.

On the other hand, encapsulation of many other drug molecules with high concentration such as anti-cancer drugs could be achieved using our developed particles and the novel rotavap method for encapsulation. Also, these could be used as a potential gene delivery system into the cells. This will make the particles as having dual functions: delivery of chemical compound (e.g. drug molecule or fluorescent dye) in addition to nucleic acids of different nature (plasmid, siRNA, miRNA…etc).

Taken together, the nanoparticle system reported here combines high surface area, high drug loading efficiency, and sustained cargo release with the potential for specific cell targeting and endosomal escape. These properties may allow for utilizing the NPs as (drug/gene) delivery system for combating infectious diseases, and cancer, by simply encapsulating any other drug molecule and/or targeting moiety for the appropriate cell type thus, minimizing the drugs side effects.

References

1. Meijer M (2001) Drug Targeting: organ-specific strategies: Methods and Principles in Medicinal Chemistry (1stedtn), Wiley-VCH, New York.
2. Kaparissides CS, Alexandridou, Chaitidou KKAS (2006) Recent advances in Novel Drug Delivery systems. Nanotechnology Online 2. Int J PharmTech Res 2: 2025-2027.
3. Slowing II, Trewyn BG, Giri S, Lin VSY (2007) Mesoporous Silica Nanoparticles for Drug Delivery and Biosensing Applications. Adv Funct Mater 17: 1225-1236.
4. Patil A, Chirmade UN, Trivedi V, Lamprou DA, Urquhart A, et al. (2011) Encapsulation of water insoluble drugs in mesoporous silica nanoparticles using supercritical carbon dioxide. J Nanomedic Nanotechnol 2: 111.
5. Liu Q, Zhang J, Sun W, Xie QR, Xia W, et al. (2012) Delivering hydrophilic and hydrophobic chemotherapeutics simultaneously by magnetic mesoporous silica nanoparticles to inhibit cancer cells. Int J Nanomedicine 7: 999-1013.
6. Lai CY, Trewyn BG, Jeftinija DM, Jeftinija K, Xu S, et al. (2003) A Mesoporous Silica Nanosphere-Based Carrier System with Chemically Removable CdS Nanoparticle Caps for Stimuli-Responsive Controlled Release of Neurotransmitters and Drug Molecules. J Am Chem Soc 125: 4451-4459.
7. Koul A, Arnoult E, Lounis N, Guillemont J, Andries K (2011) The challenge of new drug discovery for tuberculosis. Nature 469: 483-490.
8. Andries K, Verhasselt P, Guillemont J, Göhlmann HW, Neefs JM, et al. (2005) A diarylquinoline drug active on the ATP synthase of Mycobacterium tuberculosis. Science 307: 223-227.
9. Koul A, Dendouga N, Vergauwen K, Molenberghs B, Vranckx L, et al. (2007) Diarylquinolines target subunit c of mycobacterial ATP synthase. Nat Chem Biol 3: 323-324.
10. Griffiths G, Nyström B, Sable SB, Khuller GK (2010) Nanobead-based interventions for the treatment and prevention of tuberculosis. Nat Rev Microbiol 8: 827-834.
11. Ahmad Z, Pandey R, Sharma S, Khuller GK (2006) Pharmacokinetic and pharmacodynamic behaviour of antitubercular drugs encapsulated in alginate nanoparticles at two dosesd. Int J Antimicrob Agents 27: 8.
12. Zahoor A, Sharma S, Khuller GK (2005) Inhalable alginate nanoparticles as antitubercular drug carriers against experimental tuberculosis. Int J Antimicrob Agents 26: 298-303.
13. Tasciotti E, Liu X, Bhavane R, Plant K, Leonard AD, et al. (2008) Mesoporous silicon particles as a multistage delivery system for imaging and therapeutic applications. Nat Nanotechnol 3: 151-157.
14. Diebold SS, Kursa M, Wagner E, Cotten M, Zenke M (1999) Mannose polyethylenimine conjugates for targeted DNA delivery into dendritic cells. J Biol Chem 274: 19087-19094.
15. Park IY, Kim IY, Yoo MK, Choi YJ, Cho MH, et al. (2008) Mannosylated polyethylenimine coupled mesoporous silica nanoparticles for receptor-mediated gene delivery. Int J Pharm 359: 280-287.
16. Asthana GS, Asthana A, Kohli DV, Vyas SP (2014) Mannosylated chitosan nanoparticles for delivery of antisense oligonucleotides for macrophage targeting. Biomed Res Int 2014: 526391.
17. Erbacher P, Bousser MT, Raimond J, Monsigny M, Midoux P, et al. (1996) Gene transfer by DNA/glycosylated polylysine complexes into human blood monocyte-derived macrophages. Hum Gene Ther 7: 721-729.
18. Hashimoto M, Morimoto M, Saimoto H, Shigemasa Y, Yanagie H, et al. (2006) Gene transfer by DNA/mannosylated chitosan complexes into mouse peritoneal macrophages. Biotechnol Lett 28: 815-821.
19. Kawakami S, Sato A, Nishikawa M, Yamashita F, Hashida M (2000) Mannose receptor-mediated gene transfer into macrophages using novel mannosylated cationic liposomes. Gene Ther 7: 292-299.
20. Sato A, Kawakami S, Yamada M, Yamashita F, Hashida M (2001) Enhanced gene transfection in macrophages using mannosylated cationic liposome-polyethylenimine-plasmid DNA complexes. J Drug Target 9: 201-207.
21. Lai CY, Trewyn BG, Jeftinija DM, Jeftinija K, Xu S, et al. (2003) A mesoporous silica nanosphere-based carrier system with chemically removable CdS nanoparticle caps for stimuli-responsive controlled release of neurotransmitters and drug molecules. J Am Chem Soc 125: 4451-4459.
22. Slowing I, Trewyn BG, Lin VS (2006) Effect of surface functionalization of MCM-41-type mesoporous silica nanoparticles on the endocytosis by human cancer cells. J Am Chem Soc 128: 14792-14793.
23. Monsigny M, Petit C, Roche AC (1988) Colorimetric determination of neutral sugars by a resorcinol sulfuric acid micromethod. Anal Biochem 175: 525-530.
24. Meszaros R, Thompson L, Bos M, Groot PD (2002) Adsorption and electrokinetic properties of polyethylenimine on silica surfaces. Langmuir 18: 6164-6169.
25. Meszaros R, Varga I, Gilányi T (2003) Adsorption Properties of Polyethyleneimine on Silica Surfaces in the Presence of Sodium Dodecyl Sulfate. Langmuir 19: 9977-9980.
26. Mészáros R, Thompson L, Varga I, Gilányi T (2004) Adsorption of poly(ethyleneimine) on silica surfaces: effect of pH on the reversibility of adsorption. Langmuir 20: 5026-5029.
27. Braga PRS (2011) Liquid phase calorimetric-adsorption analysis of Si-MCM-41: Evidence of strong hydrogen-bonding sites. Microporous Mesoporous Mater 139: 74-80.
28. Vadia (2011) Mesoporous material, MCM 41: A new drug delivery. Asian J Pharm Clin Res 4: 44-53.
29. Marzouqa DM, Zughul MB, Taha MO, Hodali HA (2011) Effect of particle morphology and pore size on the release kinetics of ephedrine from mesoporous MCM-41 materials. J Porous Mat 19: 825-833.
30. Lu J, Liong M, Zink JI, Tamanoi F (2007) Mesoporous silica nanoparticles as a delivery system for hydrophobic anticancer drugs. Small 3: 1341-1346.
31. Zhu M, Wang H, Liu J, He H, Hua X, et al. (2011) A mesoporous silica nanoparticulate/Î²-TCP/BG composite drug delivery system for osteoarticular tuberculosis therapy. Biomaterials 32: 1986-1995.
32. Kleemann E, Dailey LA, Abdelhady HG, Gessler T, Schmehl T (2004) Modified

polyethylenimines as non-viral gene delivery systems for aerosol gene therapy: investigations of the complex structure and stability during air-jet and ultrasonic nebulization. J Control Release 100: 437-450.

33. Read ML, Bremner KH, Oupický D, Green NK, Searle PF, et al. (2003) Vectors based on reducible polycations facilitate intracellular release of nucleic acids. J Gene Med 5: 232-245.

34. Zanta MA, Boussif O, Adib A, Behr JP (1997) In vitro gene delivery to hepatocytes with galactosylated polyethylenimine. Bioconjug Chem 8: 839-844.

35. Duan H, Nie S (2007) Cell-penetrating quantum dots based on multivalent and endosome-disrupting surface coatings. J Am Chem Soc 129: 3333-3338.

36. Koul A, Herget T, Klebl B, Ullrich A (2004) Interplay between mycobacteria and host signalling pathways. Nat Rev Microbiol 2: 189-202.

37. Gomez JE, McKinney JD (2004) M. tuberculosis persistence, latency, and drug tolerance. Tuberculosis (Edinb) 84: 29-44.